Applied Catalysis B: Environmental 91 (2009) 640–648

Contents lists available at ScienceDirect

Applied Catalysis B: Environmental

journal homepage: www.elsevier.com/locate/apcatb

Silver supported mesoporous SBA-15 as potential catalysts for SCR NO_x by ethanol

Maya Boutros [a], Jean-Michel Trichard [b], Patrick Da Costa [a,*]

[a] Université Pierre et Marie Curie, Paris 6, UPMC, Laboratoire de Réactivité de Surface, UMR CNRS 7197, Case 178, 4 place jussieu, 75252 Paris 05, France
[b] Renault SAS, DREAM/DTAA, Technocentre Renault, 1 avenue du Golf, 78280 Guyancourt, France

ARTICLE INFO

Article history:
Received 18 May 2009
Received in revised form 3 July 2009
Accepted 6 July 2009
Available online 17 July 2009

Keywords:
Silver
Mesoporous silica or aluminosilica
NO_x
Ethanol

ABSTRACT

Reduction of nitrogen oxides (NO_x) in a lean exhaust gases has become one of the most important environmental concerns. This study compared the performances of $DeNO_x$ and the properties of silver/mesoporous aluminosilica synthesized by different methods. Silver nanoparticles were obtained after calcination of the materials prepared by incipient wetness or by the excess solvent impregnation of Al-SBA-15 support by silver nitrate. On the other hand, the silver nitrate was introduced on the synthesis gel of SBA-15. The solid product was used as support to deposit aluminium. The effect of synthesis method on silver incorporation and the porous structure of the resulting solids has been examined. Some techniques had been applied, such as: elemental analysis, X-ray diffraction (XRD), N_2 sorption measurements and Transmission Electron Microscopy (TEM). The nature of silver species in these catalysts was investigated by XPS measurements, high angle XRD, high resolution TEM and TPR/H_2 (temperature-programmed reduction). The resulting materials were tested in the selective catalytic reduction of NO_x by ethanol in the presence of oxygen. Finally, the effect of H_2 on the $DeNO_x$ activity was also investigated.

The impregnation method of Al-SBA-15 by silver nitrate influences the size, the location of the particles and the catalytic activity. To maintain a higher $DeNO_x$ activity, the percentage of aluminium loading and the feed of H_2 gases should be increased.

1. Introduction

Silica or aluminosilica with an hexagonal structured mesopore network (MCM-41 and SBA-15) have been extensively studied since the first report dealing with their synthesis [1,2]. Their high specific surface area, porous volume and adjustable pore size diameter make them ideal support for the preparation of highly dispersed heterogeneous catalysts [3,4]. These materials have attracted significant attention in related fields of academia and industry, and have been widely applied as catalysts in petrochemical industry. Their remarkable high surface area favoring a high dispersion of the active component on the surface of the catalytic support as well as the improved accessibility of active sites in comparison with zeolites should have a favorable impact on catalytic activity [5,6]. However, the low acidity and hydrothermal stability limited their application in the environmental catalysis, such as selective catalytic reduction (SCR) of NO in the presence of oxygen.

Nitrogen oxides (NO_x) are produced by both natural and anthropogenic sources. They contribute to a variety of environmental problems such as: the formation of acid rain, the resultant acidification of aquatic systems, ground-level ozone (smog), and general atmospheric degradation [7]. The major technology for reducing nitrogen oxide emission from stationary sources is the SCR of NO_x by ammonia.

In the family of mesoporous materials, SBA-15 materials synthesized under acidic conditions exhibit larger pore size and thicker pore volume wall compared with M41S. The improved hydrothermal and thermal stability makes them the most promising catalytic materials [2]. The introduction of Al into the structure of SBA-15 is an effective way to enhance for example its acidity which may promotes the SCR reactions [8,9].

Such mesoporous silica SBA-15 modified with copper, iron, Pt, Mn, TiO_x and VO_x oxides, were already studied in SCR of NO by ammonia [10–13]. Although the established SCR process for stationary plants is based on the reduction of NO_x by ammonia, this latter technology is not so easy to implement on automotive field due to difficulties in the storing or handling of NH_3. Extensive research is necessary to discover alternative catalytic systems for mobile NO_x source where these molecules such as hydrocarbons are more acceptable for the environment and they can be used for the reduction [14–16]. It is well known that transition metal ion exchanged zeolites, in particular Cu-ZSM-5, show high HC-SCR activity [17]. The most transition metal zeolites catalyst (cobalt,

* Corresponding author. Tel.: +33 1 44 27 55 12; fax: +33 1 44 27 60 33.
E-mail address: patrick.da_costa@upmc.fr (P. Da Costa).

0926-3373/$ – see front matter © 2009 Elsevier B.V. All rights reserved.
doi:10.1016/j.apcatb.2009.07.004

palladium, rhodium, iron, silver, cerium, gallium, indium and manganese) show the advantage of reducing NO_x selectively into N_2, in contrast to e.g., platinum based catalysts on which N_2O formation can be significant [18]. Due to the poor hydrothermal stability and low acidity of transition, metal ions exchange zeolites in the presence of H_2O and SO_2 [19]. However, they are unlikely to become practical catalysts for lean NO_x abatement. The HC-SCR methods have been studied in the presence of transition metals (such as Pt, Rh and Co) supported on mesoporous molecular sieves with MCM-41 type structure [19–21].

Among the different active phases studied for NO_x reduction, alumina supported silver-based catalysts (Ag/Al_2O_3) have shown good results using either hydrocarbons or oxygenated compounds (same alcohol) as reducing agents [22–26]. Alcohol was mixed in gasoline as fuel for automotive vehicles and that was better for control of air pollution. The addition of ethanol reduces the emission of olefins, aromatics, complex hydrocarbons and SO_x [27].

The selectivity of catalysts to nitrogen (N_2) and the formation of undesired N_2O depend on both the nature of the active component and the surface properties of the support [28,29].

The aim of this paper is to reach a better dispersion of the silver particles on mesoporous silica or aluminosilica and test their reactivity for SCR NO_x using ethanol as reducing agent. We study the influence of the impregnation method on the physico-chemical properties, the morphology of silver nanoparticles and catalytic performances of mesoporous supported silver catalysts.

In this work, silver/Al-SBA-15 materials were synthesized, characterized by various techniques and used in the $DeNO_x$ reaction of the SCR process by ethanol. Two types of Ag-Al-SBA-15 were prepared. First, we incorporated Al into SBA-15, and then Ag was impregnated on Al-SBA-15 by using two methods: excess solvent impregnation (ESI) and incipient wetness impregnation (IWI). Second, the sample was prepared by introducing the silver in the gel of SBA-15 and then impregnated after calcination by aluminium nitrate. The properties and catalytic activity of the selective reduction of NO_x with ethanol in Lean Burn Conditions were investigated.

2. Experimental

2.1. Chemicals

The different reagents, i.e. Pluronic 123 (EO_{20} PO_{70} EO_{20}, M_{av} = 5800, Aldrish), tetraethyl orthosilicate (TEOS, Fluka), tetramethyl orthosilicate (TMOS, Fluka), isopropoxide aluminium (Acros), nitric acid (HNO_3, 68%, Prolabo), 37 wt% fuming hydrochloric acid (HCl, SDS), aluminium nitrate nonahydrate (98+%, Aldrich), silver nitrate (99.9%-Ag, Strem chemicals) were used as received.

2.2. Mesoporous Ag-Al-SBA-15 materials synthesis

2.2.1. Al-SBA-15 as support of catalyst

Two methods of synthesis of Al-SBA-15 were described, with a theoretical molar ratio (Si/Al) about 10:6:

(a) The mesoporous aluminosilica Al-SBA-15 (10) was synthesized using a hydrothermal method described by Li et al. [30] with the theoritical molar ratio Si/Al of 10. This support was prepared by dissolving 4 g of P123 in 150 mL of aqueous HCl at pH 1.5 (solution A). Then 6.4 mL of TMOS and 0.88 mL of isopropoxide aluminium were added to 10 mL of aqueous HCl at pH 1.5 (solution B). Solution B was stirred at room temperature (RT) for about 3 h and then added dropwise to solution A. The resulting mixture was aged for 20 h at 40 °C and then transferred into an autoclave at 100 °C for 24 h. The product was filtred, washed, dried and calcined at 550 °C for 5 h.

(b) Other mesoporous aluminosilica support Al-SBA-15 (6) was synthesized with a theoretical molar ratio Si/Al of 6. This solid was obtained by excess solvent impregnation of the SBA-15 silica with an aluminium nitrate aqueous solution. This suspension was stirred and heated at (60 °C) under low vacuum conditions in order to evaporate water in mild conditions. After 2 h of maturation at RT, the solid was dried overnight at 120 °C and then the product was calcined at 550 °C for 5 h.

2.2.2. Ag-SBA-15 as support of catalyst

A mesoporous Ag-SBA-15 material was synthesized by direct hydrothermal synthesis [31]. The theoretical loading of silver introduced was about 2.5 wt%. The process was as follows: 4 g of P123 were dissolved in a mixture of 120 mL of distilled water and 12 g of nitric acid for 3 h at 40 °C. Silver nitrate (0.2 g) was introduced into the solution which was stirred until it became clear. Then 9 mL of TEOS were slowly added. The solution was stirred for 20 h at 40 °C and the silica gel was aged for 24 h at 100 °C. The resulting solid obtained after filtration, Ag-SBA-15, was calcined at 550 °C for 5 h. Based on the results obtained, another solid was prepared with 1.3 g of silver nitrate introduced in the gel of synthesis of SBA-15.

The solids were named Ag(x)/SBA-15, x is the real percentage of silver obtained after calcination.

2.2.3. Ag-Al-SBA-15 catalysts

(a) The catalyst Ag/Al-SBA-15 (10) (ESI) was prepared by excess solvent impregnation of the Al-SBA-15 (10) with an $AgNO_3$ aqueous solution. This suspension was stirred and heated under low vacuum conditions in order to evaporate water in mild conditions.
(b) The catalyst Ag/Al-SBA-15 (10) (IWI) was synthesized by incipient wetness impregnation. The silver containing aqueous solution (1.1 mL) is added to 1 g of Al-SBA-15 support.
(c) The catalyst Ag/Al-SBA-15 (6) (ESI) was prepared by ESI, using Al-SBA-15 (6) support and $AgNO_3$ aqueous solution.

The theoretical loading of silver is 2.5 wt% in the (a)–(c) cases.

(d) The Al/Ag-SBA-15 solid was synthesized by ESI of the Ag-SBA-15 support and aluminium nitrate aqueous solution. The theoretical molar ratio of Si/Al is 10.

After 2 h of maturation at RT, all the catalysts (a–d) were dried 2 h at RT, and then overnight at 120 °C. These solids were calcined under air flow at 500 °C for 2 h.

Table 1 summarizes the catalysts samples silver/mesoporous aluminosilica and their method of synthesis.

2.3. Catalyst characterization

The catalysts were characterized by X-ray diffraction (XRD), temperature-programmed reduction (TPR) measurements, N_2 sorption, transmission electronic microscopy (TEM) and X-ray

Table 1
Preparation method for Ag-Al-SBA-15 catalysts.

Catalysts	Supports	Synthesis method
Ag/Al-SBA-15 (10) (IWI)	Al-SBA-15 (10)	Incipient wetness impregnation (IWI)
Ag/Al-SBA-15 (10) (ESI)	Al-SBA-15 (10)	Excess solvent impregnation (ESI)
Ag/Al-SBA-15 (6) (ESI)	Al-SBA-15 (6)	Excess solvent impregnation (ESI)
Al/Ag-SBA-15 (ESI)	Ag-SBA-15	Excess solvent impregnation (ESI)

spectroscopy (XPS). Silver, aluminium and silicon composition of the various materials were determined by elemental analysis (ICPAES) in the CNRS center at Vernaison (France).

XRD data were recorded on a Bruker Advanced D8 using CuKα radiation. PXRD measurements were performed from 0.5° to 5° (2θ) in steps of 0.02° with a count time of 6 s at each point. XRD data (from 10° to 70° (2θ)) was carried out on a Siemens model D-500 diffractometer with CuKα radiation. XPS spectra were obtained on a SPECS PHOIBOS 100 spectrometer equipped with a MgKα X-ray source.

Redox properties were studied by TPR using a TPD/R/O instrument (ThermoQuest) which consists of a cylindrical quartz microreactor, coupled with a gas chromatograph equipped with a thermal conductivity detector (TCD). The treatment of the solid (50 mg) was carried out in a He gas flow (20 mL/min) at room temperature. The thermoreduction process was performed by passing a 5% H_2/Ar gas mixture (20 mL/min) through the sample while heating from 40 to 500 °C (ramping rate 10 °C/min). The final temperature was kept at 500 °C for 30 min. N_2 adsorption–desorption isotherms were measured at liquid nitrogen temperature by a Micromeritics ASAP 2010. Before the measurements, the samples were evacuated at 200 °C under vacuum (2×10^{-3} Torr). The pore diameter and specific pore volume were calculated according to the Barrett–Joyner–Halenda (BJH) model. The specific surface area was obtained by using the Brunauer–Emmett–Teller (BET) equation.

High resolution TEM (HRTEM) was performed on a JEOL-JEM 2011 HR (LaB) microscope operating at 200 kV.

2.4. Catalytic measurements

Temperature-programmed surface reaction (TPSR) and steady-state experiments were carried, in a U-type glass reactor by using gas mixture consisting of 500 ppm NO + 2500 ppm C_2H_5OH + 10% O_2 in Ar. The gas hourly space velocity was fixed: GHSV = 21,766 h^{-1}. The gases (NO, O_2 and Ar) were fed from compressed cylinders provided by Air Liquide and adjusted with Brooks mass flow controllers (5850 TR and 5850 TE). Ethanol was supplied to the reacting stream by means of two temperature-controlled bubble towers (purged by Ar flow): a saturator at RT and a condenser at −5 °C. The total flow rate of the feed gas was maintained at 250 mL/min for all experiments. The sample (90 mg) was held on plugs of quartz wool and the temperature was controlled through a EUROTHERM 2408 temperature controller using a K-type thermocouple. The composition of the reactor outflow was continuously measured using a set of specific detectors. An Eco Physics CLD 700 AL chemiluminescence NO_x analyser (for NO and total NO_x (i.e. NO + NO_2)) allowed the simultaneous detection of NO and NO_x. Two Ultramat 6 IR analysers were used to monitor N_2O, CO and CO_2. A FID detector (Fidamat 5) was used to follow the concentration of the hydrocarbonated compounds.

3. Results and discussion

3.1. Characterization of the support and active phase

Aluminium insertion through the co-condensation technique was partial (Si/Al obtained is 13 instead of 10). We can note that all the amount of aluminium introduced by impregnation is retained. The molar ratio Si/Al obtained after impregnation of SBA-15 by aluminium nitrate is equal to the theoretical value (Table 2).

Elemental analyses results show that the silver content of the solid obtained from Al-SBA-15 (10) by excess solvent impregnation is 2.4 wt% (Table 2). This value is twice than those of Ag/Al-SBA-15 (IWI) (2.1 wt%).

Table 2
Physicochemical properties of the samples.

Code	Sample	Si (wt%)	Al (wt%)	Ag (wt%)
Al(10)	Al-SBA-15 (10)	33.9	2.5	–
Ag/Al(10)I	Ag-Al-SBA-15 (10) (IWI)	35.5	2.7	2.1
Ag/Al(10)E	Ag-Al-SBA-15 (10) (ESI)	34.9	2.7	2.4
Al(6)	Al-SBA-15 (6)	35.4	5.2	–
Ag/Al(6)E	Ag/Al-SBA-15 (6) (ESI)	35.0	4.6	2.5
Ag(0.3)	Ag(0.3)-SBA-15	41.0	–	0.3
Al/Ag(0.3)	Al/Ag(0.3)-SBA-15 (ESI)	38.2	2.6	0.2
Ag(2.5)	Ag(2.5)-SBA-15	38.0	–	2.4
Al/Ag(2.5)	Al/Ag(2.5)-SBA-15	36.5	2.6	2.4

For 2.5 wt% theoretical value of Ag, just 12% of silver introduced in the gel of synthesis of SBA-15 is retained. It is very difficult to introduce the metal ions into SBA-15 directly due to the difficulties in the formation of metal–O–Si bonds under the strong acidic conditions for the synthesis of SBA-15 materials [32,33]. For this reason, to obtain 2.5 wt% real percentage of silver, another solid Ag-SBA-15 was synthesized by introducing a big amount (1.3 g) of metal salt in the synthesis gel.

Fig. 1 shows that both Al-SBA-15 (10) and Ag/Al-SBA-15 (10) have very similar patterns with three well-resolved characteristic diffraction peaks which are attributed to 100, 110 and 200 of hexagonal structure (Fig. 1A). The diffraction peaks of Ag/Al-SBA-15 (10) (ESI) were shifted to slightly lower values than those of Al-SBA-15 (10) and Ag/Al-SBA-15 (10) (IWI). This difference may be related to the method of incorporation of silver particles inside the pores of aluminosilica materials. The Ag-SBA-15 prepared by direct hydrothermal synthesis was characterized by an hexagonal structure despite the addition of silver in the synthesis gel (Fig. 1B). The addition of aluminium to Ag-SBA-15 does not modify the hexagonal structure of the support.

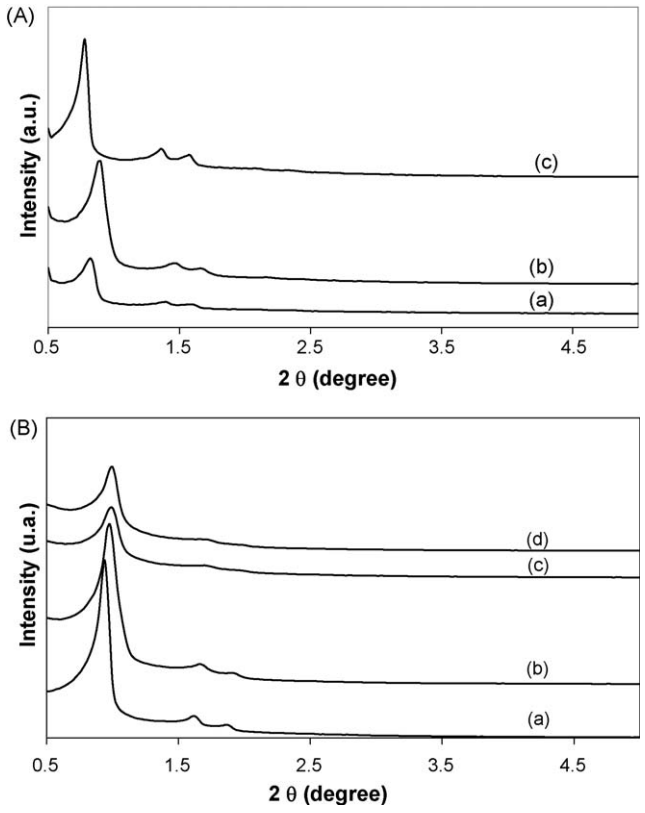

Fig. 1. Small angle X-ray diffraction patterns of (A): (a) Al(10), (b) Ag/Al(10)I and (c) Ag/Al(10)E; (B): (a) Ag(0.3), (b) Al/Ag(0.3), (c) Ag(2.5) and (d) Al/Ag(2.5).

Table 3
Textural properties of the samples and metallic silver content determined by XPS analysis.

Code	S_{BET} ($m^2\ g^{-1}$)	V_{pores} ($cm^3\ g^{-1}$)	D_{pores} (nm)	Metallic silver content by XPS (%)
Al(10)	818	1.1	8.2	–
Ag/Al(10)I	730	0.99	7.5	85
Ag/Al(10)E	704	1.00	7.5	78
Al(6)	613	0.86	6.3	–
Ag/Al(6)E	480	0.72	6.4	77
Ag(0.3)	963	1.2	5.8	26
Al/Ag(0.3)	745	0.96	5.4	72
Ag(2.5)	723	0.72	5.1	–
Al/Ag(2.5)	570	0.61	5.1	–

As expected, the increase of silver loading leads to the gradual decrease of the intensities of each peak. Indeed the reflections corresponding to the (1 1 0) and (2 0 0) planes cannot be easily discerned for Al/Ag(2.5)-SBA-15. This indicates that the sample is less structured than the other samples (Fig. 1B).

The textural properties of the Ag-Al-SBA-15 samples prepared with different methods of synthesis are listed in Table 3. It appears that the specific surface area and pore volume of Ag/Al-SBA-15 (10) (ESI) and (IWI) are very similar to those of the pure aluminosilica material Al-SBA-15 (10). When the Si/Al molar ratio decreases, the textural properties decrease (±∼20%), it is the case of the catalyst Ag/Al-SBA-15 (6) (ESI) and its support. Nitrogen adsorption–desorption isotherms of Ag-Al-SBA-15 (ESI) and (IWI) are still characteristic of Al-SBA-15 material used as support (Fig. 2A).

N_2 adsorption–desorption isotherms of Ag-SBA-15 exhibit characteristic type IV isotherms with a H1 hysteresis loop as defined by IUPAC (Fig. 2A). The steep increases of the adsorption volume at P/P_0 (0.5–0.7) are due to capillary condensation of nitrogen in the mesopores. The hysteresis loops become smaller but wider with increasing amount of silver (case of Ag(2.5) and Al/Ag(2.5)). This is a perturbation due to the incorporation of big amount of metal. The sample prepared by direct hydrothermal synthesis (Ag(0.3)-SBA-15) is characterized by a high specific surface area (∼900 $m^2\ g^{-1}$, Table 3). The amount of silver retained by direct synthesis, roughly 0.3 wt%, is too small to observe a significant decrease in the specific surface area and in the pore volume that could be related to the presence of particles inside the pores channels [34]. However, more significant decreases of the textural parameters are observed in the case of Ag(2.5)-SBA-15 (Table 3). There are the result of the perturbations of the self-assembly of surfactant agregates due to the incorporation of bigger amount of metal during the co-condensation process [35]. From the XRD patterns and N_2 sorption, we can conclude that the incorporation of silver nitrate in the synthesis gel of SBA-15 never destroy the mesoporous and hexagonal structure. The excess solvent impregnation of Ag-SBA-15 support by aluminium nitrate (∼2.5%) causes a decrease of the specific area and of the pore volume (−20%) (Table 3).

Fig. 2B shows a typical BJH pore size distribution of the support and of the catalysts based silver. The method of preparation of Ag/Al(10)I or E, the impregnation of Al-SBA-15 (10) by silver leads to a decrease in the mean pores diameters from 8.2 to 7.5. The variation of the theoretical molar ratio Si/Al from 10 to 6 leads to a decrease in the pores diameters from 8.2 to 6.3 nm.

The pore size distribution of Ag-SBA-15 sample is centered on 5.8 nm (Ag(0.3)) and 5.1 nm (Ag 2.5)). For Ag(0.3)-SBA-15, this distribution is narrower to Al-SBA-15 and Ag-Al-SBA-15 materials.

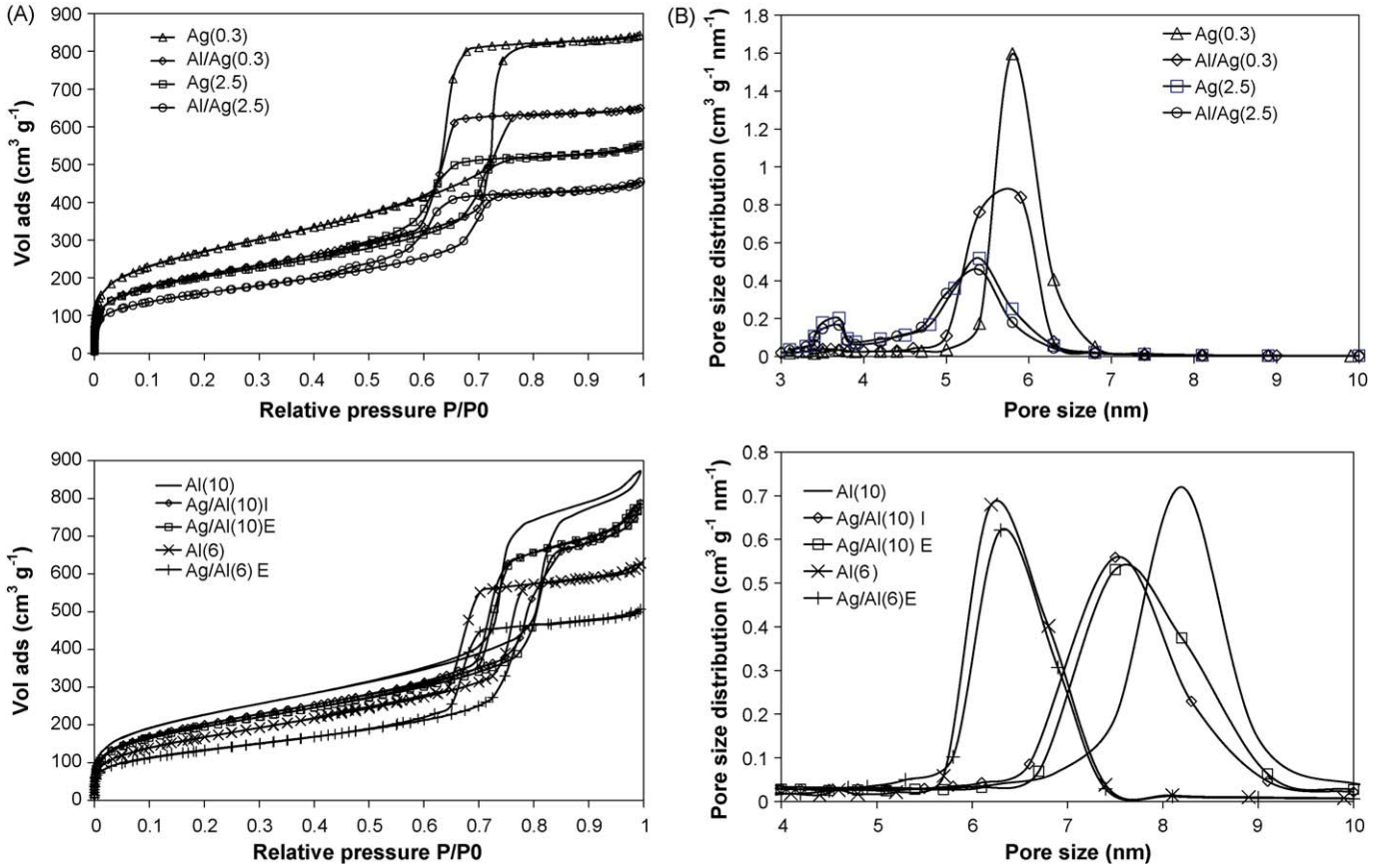

Fig. 2. (A) N_2 adsorption–desorption isotherms at 77 K of mesoporous silica and aluminosilica based catalysts. (B) Pore size distribution curves of mesoporous silica and aluminosilica based catalysts.

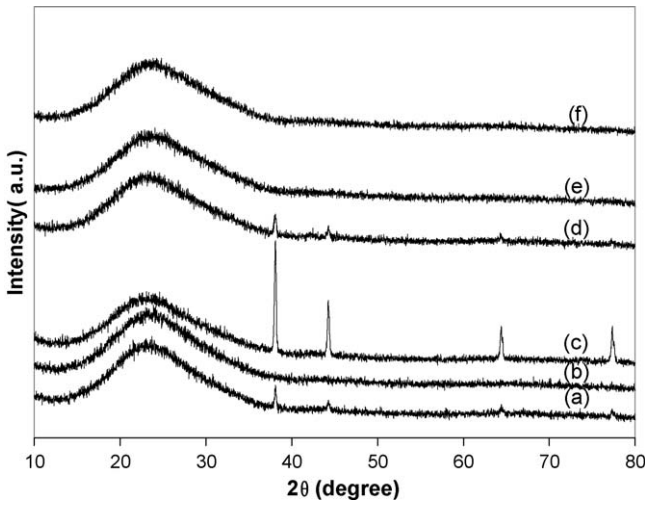

Fig. 3. High angle X-ray diffraction pattern of (a) Ag(0.3), (b) Al/Ag(0.3), (c) Ag(2.5), (d) Al/Ag(2.5), (e) Ag/Al(10)E and (f) Ag/Al(10)I.

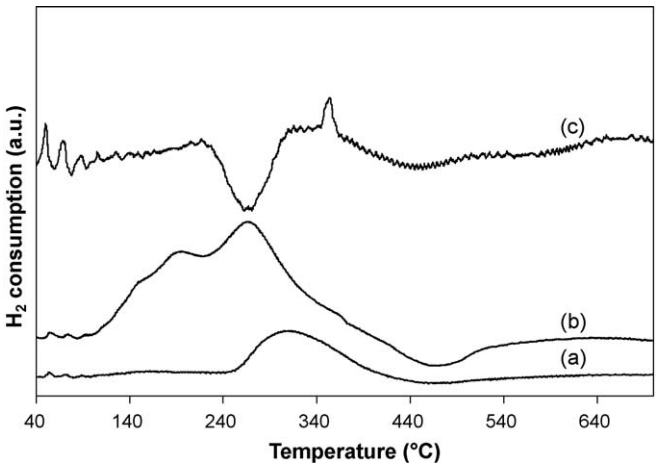

Fig. 4. H_2-TPR profiles of (a) Ag/Al(10)I, (b) Ag/Al(10)E and (c) Al/Ag(0.3).

The addition of aluminium nitrate to Ag-SBA-15 does not cause a significant change of pore diameter.

The high angle XRD patterns of the calcined silver/mesoporous aluminosilica were shown in Fig. 3. For all the samples, a broad peak at about $2\theta \approx 22^\circ$ is ascribed to the amorphous silica. For the samples prepared by impregnation of Al-SBA-15 (10) by silver nitrate, no peaks corresponding to Ag°, Ag_2O or $AlAgO_2$ phases were observed (Fig. 3(e) and (f)).

Four very intense diffraction peaks, which correspond to the (1 1 1), (2 0 0), (2 2 0) and (3 1 1) lattice planes of the cubic structure of Ag° were observed, respectively, in the case of Ag-SBA-15 obtained by direct synthesis (JCPDS: 03-065-2871) (Fig. 3(a) and (c)). The intensities of these peaks decrease when the amount of silver decreases. However, when 2.5% of aluminium were added to the Ag-SBA-15 support by excess solvent impregnation (Fig. 3(b) and (d)), the detection of the peaks corresponding to the metallic silver became difficult.

The size of crystallites was estimated using the Scherrer formula. However, this method is not precise because not all crystallites have the same size. For the sample Ag(2.5), the estimated size of particles is about 40 nm.

XPS measurements were performed in order to determine the oxidation state of silver of supported catalysts Ag-Al-SBA-15. In the case of silver, the deconvolution of the $3d_{5/2}$ peak shows the presence of two contributions (367.5 and 368.5 eV), which are attributed, according with the literature [36], mainly to Ag_2O and Ag°, respectively. The quantitative analysis has been performed in order to establish the content of the metallic phase. Results are presented in Table 3. For the samples prepared by impregnation of Al-SBA-15 by silver nitrate, the methods of impregnation (ESI or IWI) have a slight influence upon the reduction degree of the analyzed samples. The metallic silver content is slightly higher for the catalyst synthesized by incipient wetness impregnation. For the Ag(0.3)-SBA-15 sample prepared by direct hydrothermal synthesis, the percentage of Ag° detected by XPS is however very low (26%). The impregnation of the solid by aluminium enhances this value (case of Al/Ag(0.3)-SBA-15).

We can suppose that a part of metallic silver detected by XPS was reduced during the XPS experiments which could be related to the silver photoreduction process.

The TPR/H_2 profiles for Ag/Al-SBA-15 (10) (ESI), (IWI) catalysts are reported in Fig. 4(a and b). The different solids are reduced at a temperature lower than 440 °C. The reduction profiles for Ag/Al-SBA-15 (IWI) were characterized by a mean peak at 312 °C. For Ag/Al-SBA-15 synthesized by excess solvent impregnation, three peaks were observed: a mean at 266 °C, two minors at 150 and 195 °C, respectively. This main H_2 consumption peak is attributed to the reduction of Ag_2O clusters, the shoulder at 150 and 195 °C is due to Ag^+ cations reduction [26]. The occurrence of many peaks can also be interpreted by differences in the location, in the size of particles and/or the interaction of these particles with the support. In the case of Al/Ag(0.3)-SBA-15 (ESI), a peak located at 350 °C was observed. Moreover, a negative one at 270 °C was detected (Fig. 4(c)). The sample in which the silver was impregnated is easier to reduce compared to the silver that was introduced in the gel of synthesis. The reduction at 350 °C was followed by a water desorption, which is not the case of lower temperature [26].

Since the presence of aluminium and silver was dectected by EDS; this lack of visibility confirms the good dispersion of silver particles upon the support. The method of synthesis clearly revealed a difference in the size and location of the metal. In all cases, TEM images indicate that channels are still structured despite the introduction of metal (aluminium or silver) in the gel of synthesis of mesoporous silica SBA-15.

The incipient wetness impregnation leads to a very poor dispersion of the silver particles. TEM micrographs of Ag/Al-SBA-15 (10) (IWI) indicate that a larger particles or aggregates are also observed on the external surface (Fig. 5(a)). More nanoparticles are located in the pores of Ag/Al-SBA-15 (10) (ESI) than on the external surface (Fig. 5(b)).

Dispersed silver nanoparticles are mainly located inside the pore channels in the case of Al/Ag-SBA-15 because Ag-SBA-15 was used as raw support (Fig. 5(c) and (d)). We can note that the solid containing 2.5% of metal (Al/Ag(2.5), Fig. 5(d)), is characterized by a good dispersion of silver nanoparticles smaller than 5 nm. These results are not in agreement with those obtained by Scherrer's formular (about 40 nm). If this formula is used, the calculated value of the cristallite size changes depending on the used diffraction peak. Large variation needs to be noted. This happens because peak broadening increases with the diffraction angle and the effect of strain variance on the peak broadening is not considered [37]. For this reason TEM analyses, which one is more precise, are often used to calculate the size of the particles. HRTEM was performed to identify the location and the size of the silver particles on support and to check their dispersion. HRTEM analyses revealed fewer particles with a 4 nm-mean diameter (Fig. 5(e)). The average size of the nanoparticles is smaller than the pore aperture. For all the samples analyzed by HRTEM, the particles reticular distance was measured (about 2.4 Å) and its seem to correspond to the (1 1 1) plane of metallic silver (JCPDS: 03-065-2871).

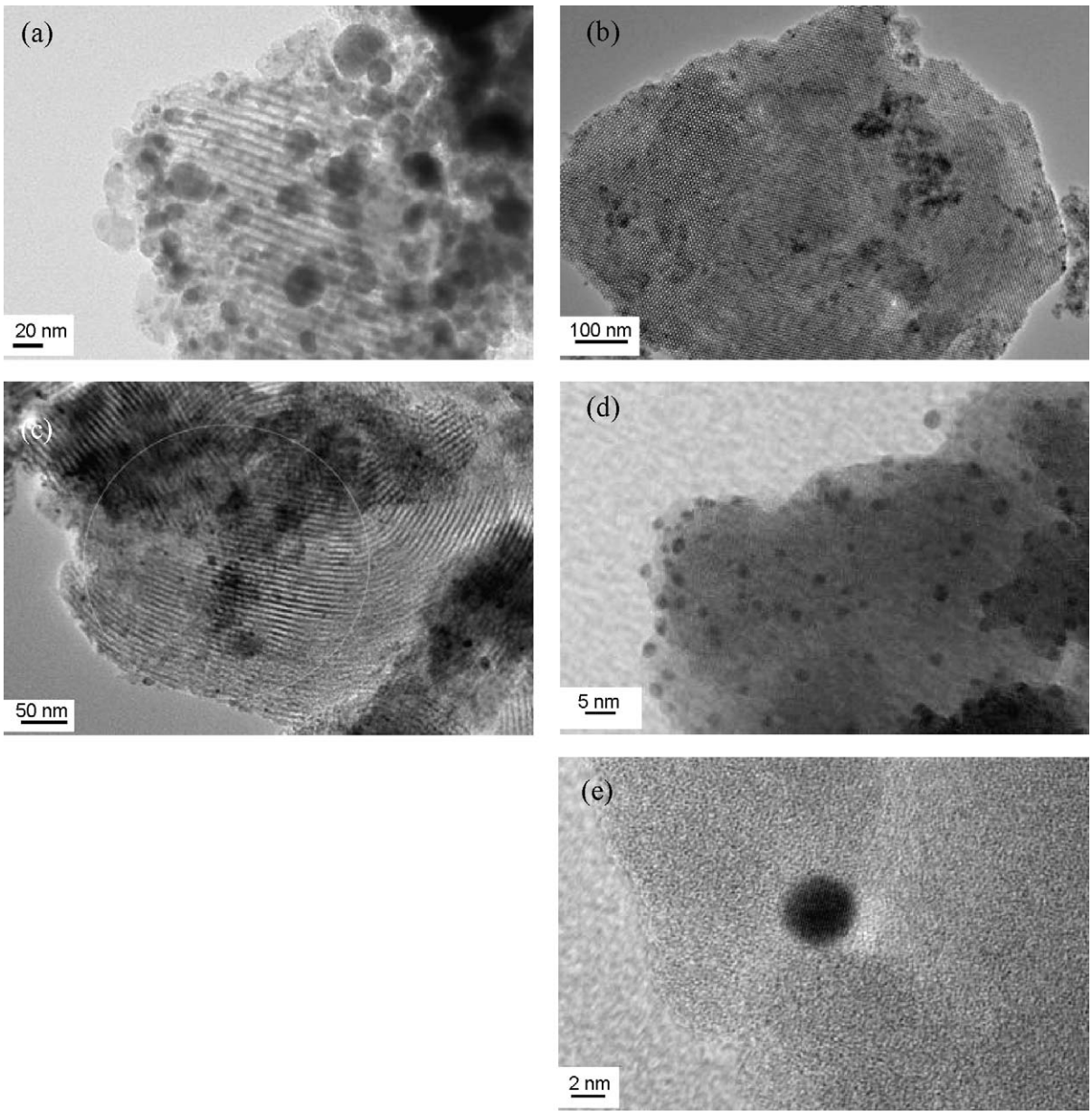

Fig. 5. TEM images of (a) Ag/Al(10)I, (b) Ag/Al(10)E, (c) Al/Ag(0.3), (d) Al/Ag(2.5) and (e) HRTEM of Al/Ag(0.3).

3.2. SCR of NO_x by ethanol

In order to compare the influence of preparation, selective reduction of NO_x runs was carried out using the following feed: 500 ppm NO + 2500 ppm C_2H_5OH + 10% O_2 in Ar. NO_x conversion as function of temperature is presented in Figs. 6–8. In all the experiments, no N_2O was detected and only nitrogen was observed as product. Except for the Al(10) and SBA-15 samples, the plots for NO_x reduction are typical volcano plots. The NO_x reduction curves pass through a maximum depending on the competition between total oxidation of ethanol by O_2 and its oxidation by NO.

First, we studied the influence of impregnation on catalytic activity. Thus, two catalysts were prepared by incipient wetness impregnation or by excess of precursor solution. For the samples prepared using Al-SBA-15 (10) as support, the conversion of NO_x to N_2 and ethanol into CO and CO_2, depends on the method of impregnation of mesoporous aluminosilica by silver nitrate (ESI or IWI). The maximum of conversion of NO_x to N_2 was found with Ag/Al-SBA-15 (10) (ESI) prepared by excess solvent impregnation, it is less to 50%. This sample remains more active at low temperatures than Ag/Al-SBA-15 (10) (IWI) but the catalytic activity is similar at high temperature (Fig. 6). These two samples contain approximately the same amount of silver obtained by elemental analyses and the same percentage of metallic phase detected by XPS measurements, the difference in the catalytic activity at low temperature is related to the particle size and their location in the pores. The low activity of Ag/Al (10)I, prepared by incipient wetness impregnation, is linked to the aggregates of silver dispersed on the external surface of support and already shown on the images of MET (Fig. 5(a)).

Moreover, Ag/Al-SBA-15 (10) (ESI) leads to oxidation of ethanol superior to that obtained in the presence of Ag/Al-SBA-15 (10) (IWI) (Fig. 6B). Thus, the influence of the method of synthesis on the catalytic activity is again evident. These results are similar to those obtained on silver supported on other supports such as alumina prepared by the same methods IWI and ESI, respectively.

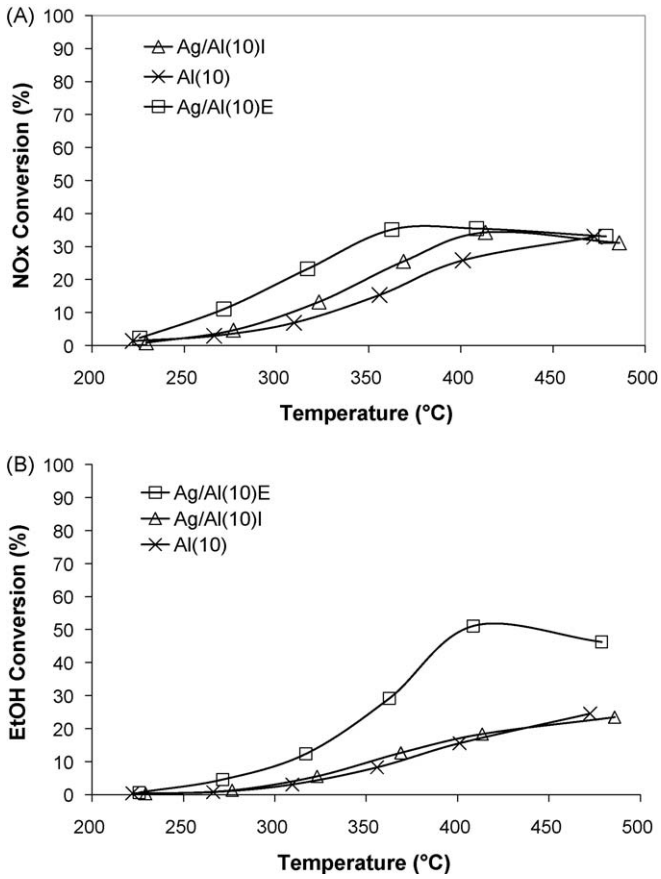

Fig. 6. (A) Steady-state NO_x conversion as function of temperature; (B) steady-state EtOH conversion into CO and CO_2 as function of temperature for catalysts prepared by incipient wetness impregnation (IWI) or in excess of solution (ESI), with Si/Al = 10.

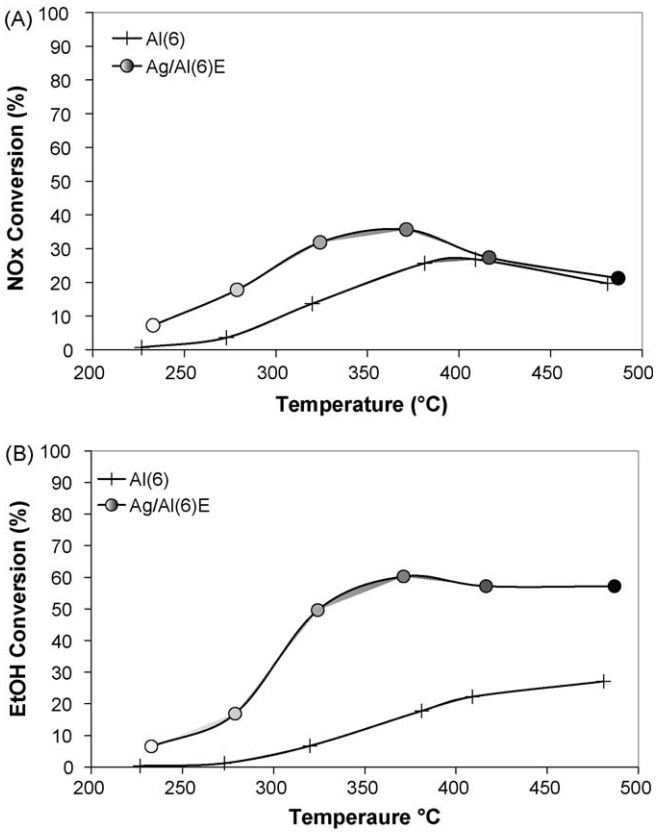

Fig. 7. (A) Steady-state NO_x conversion as function of temperature; (B) steady-state EtOH conversion into CO and CO_2 as function of temperature for catalysts with Si/Al = 6.

In that case the samples prepared by ESI demonstrate at the same temperature a higher NO_x reduction activity compared with those synthesized by incipient wetness impregnation [38].

Second, we studied the influence of the Si/Al ratio on the catalytic activity of NO_x reduction. It is well known that the best supports for such a reaction are alumina-based supports [39]. Then, we expected an increase of catalytic properties if we modify the raw SBA-15. When we increase the amount of aluminium (molar ratio Si/Al = 6), the conversion of NO_x increases at low temperatures $T \leq 350\,^{\circ}C$ (Fig. 7). This behavior is noticed in the case of Ag/Al(6) ESI and its support. For example, at $T \sim 300\,^{\circ}C$, NO_x conversions pass from 23% (Ag/Al-SBA-15 (10)) to 32% (Ag/Al-SBA-15 (6)). We can note that the presence of Al is very important to increase the selectivity of N_2 at low temperature. The Al incorporation leads to a surface modification presenting higher acidic properties [40].

As Ag/Al(6)E and Ag/Al(10) samples, prepared by excess solvent impregnation of Al-SBA-15 support, contain the same percentage of silver (~2.5%), similar dispersion, particles size (~4 nm, Figures MET not shown) and the same percentage of Ag° detected by XPS is obtained, the difference of catalytic activity is related to the presence of significant amount of aluminium and a stronger interaction metal-support for the Ag/Al(6) catalyst. One can conclude that to keep a higher $DeNO_x$ activity at low temperature; we must increase the percentage of aluminium on the mesoporous support.

Finally, we study the influence of support preparation on NO_x catalytic conversion. Thus, two supports were prepared. The first one consisted on Ag-SBA as support. The silver was introduced during the support preparation. The second one was Al SBA in which aluminium was introduced during the synthesis. For this study, two loadings of silver were considered. The results are reported in Fig. 8. Whatever the amount of silver (0.3 wt% or 2.5 wt%), the Ag-SBA-15 support synthesized by direct hydrothermal synthesis, is less active in the reduction of NO_x to N_2, however this sample leads to a better oxidation of ethanol into CO and CO_2 (100% at 400 °C) (Fig. 8). It is seen that the addition of 2.5% of aluminium to Ag-SBA-15 support enhances to the reduction of NO_x to N_2 but decreases the oxidation of ethanol to CO and CO_2 at high temperature (Al/Ag(0.3)). The XPS analyses of these samples showed that Al/Ag(0.3) contains higher metallic silver (Ag°) than Ag(0.3) (Table 3). According to the literature [39,41], the presence of silver metallic in a large proportion is necessary to increase the conversion of NO_x to N_2. For Ag/Al_2O_3 catalysts, these authors demonstrate the absence of catalytic activity when the silver is mainly present in its oxidized form.

Comparing the two catalysts Al/Ag(0.3) and Al/Ag(2.5), one can see that, at low temperature the level of NO conversion increased with increasing Ag loading in the gel of synthesis of mesoporous silica SBA-15, but avoiding an important loss of activity at higher temperatures.

The low activity of Al/Ag(0.3)-SBA-15 (ESI), compared to the Ag/Al-SBA-15 (10) (ESI), is related to the low amount of silver on these of the materials synthesized by using Ag-SBA-15 as support. However, these two catalysts are characterized by a good dispersion of particles. Indeed, we found approximately similar size of silver nanoparticles and metallic phase. For the same percentage of silver (2.5 wt%) and aluminium (~2.6 wt%), the catalytic activity of the solids prepared by ESI (Ag/Al(10)E) is similar to direct synthesis method (Al/Ag(2.5)).

Then, it is very difficult to compare the catalysts, because the catalytic activity is not just related to the particle size and/or the percentage of metal, but to the location of silver particles in the

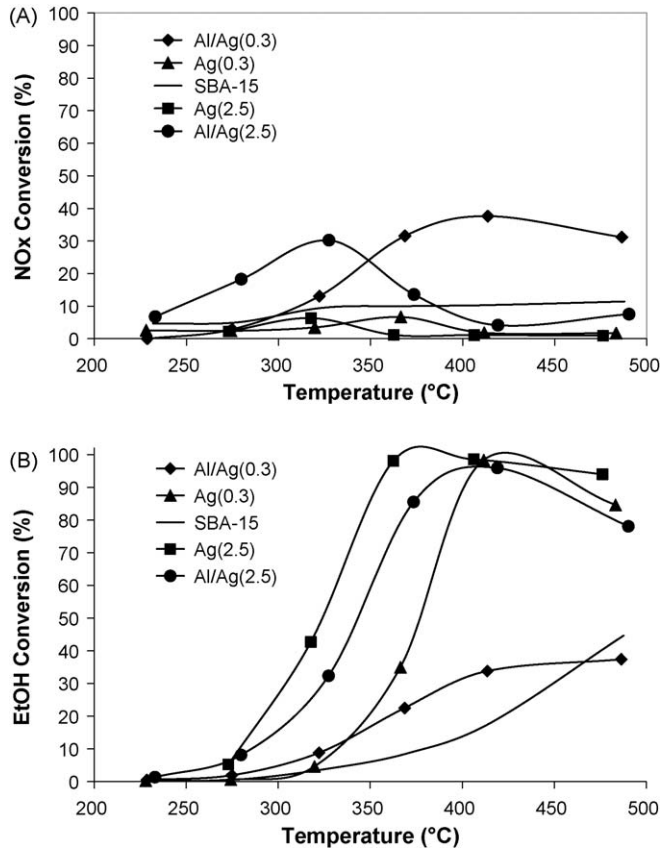

Fig. 8. (A) Steady-state NO_x conversion as function of temperature; (B) steady-state EtOH conversion into CO and CO_2 as function of temperature for catalysts prepared in direct synthesis.

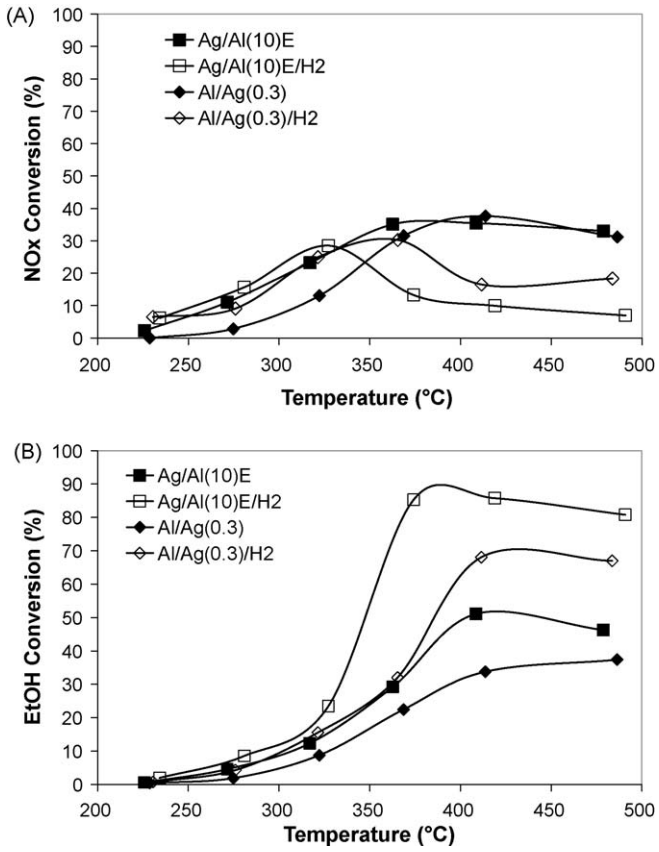

Fig. 9. (A) Steady-state NO_x conversion as function of temperature; (B) steady-state EtOH conversion into CO and CO_2 as function of temperature in absence and in presence of 1% of H_2.

pores or in the framework of mesoporous solid. In principle, the method of impregnation should lead to a dispersion of metal on the surface of mesopores, but ions incorporated in the gel of synthesis should be located in the framework of silica.

Finally, as hydrogen can be found in the exhaust gases or generated on board, the effect of H_2 on the activities of catalysts Ag/Al-SBA-15 (10) (ESI) and Al/Ag(0.3)-SBA-15 (ESI) was also investigated (Fig. 9A and B). In the presence of Ag/Al(10) prepared by ESI, when 1% of H_2 was added, the maximum NO conversion increases slightly at low temperature. On the other hand, at higher temperature, the catalytic activity decreases significantly. In the case of Al/Ag(0.3)-SBA-15, the same results were obtained (Fig. 9A). These results are comparable to those obtained in the presence of Ag/Al_2O_3 and the H_2 addition led to a high activity at lower temperature [42]. Both samples Ag/Al(10) and Al/Ag(0.3) were analyzed by XPS after catalytic activity in the presence of H_2. A quantitative analyze has been performed in order to establish the content of metallic phase. The metallic silver content is around 100% for each sample. One can suppose that the increase of N_2 conversion at low temperature is due to a higher metallic silver content in the system. These results are in agreement with those already proposed by Meunier et al. [43] on Ag/Al_2O_3 catalysts. These authors demonstrate that the metallic silver promotes the reduction of NO_x at low temperatures and enhances the oxidation of reducing agent.

In the presence of H_2, It is seen that the oxidation of ethanol into CO and CO_2 is enhanced (Fig. 9B). It can be proposed, that H_2 addition in the feed cases, increases the amount of Ag°, and thus enhances the NO_x conversion at low temperature and the ethanol oxidation. Since the presence of metallic silver is a key to the best SCR activity under such conditions, the Ag/Al-SBA-15 (10) (ESI) sample was reduced under H_2 at 500 °C before catalysis runs and used for SCR NO_x by ethanol. In steady-state conditions, no differences in conversion of NO_x have been observed. We can propose that maybe metallic silver could be covered by oxygen species during the catalytic runs as already reported elsewhere [26].

4. Conclusions

Novel catalysts for SCR NO_x by ethanol were synthesized by depositing Al on Ag-SBA-15 or Ag on Al-SBA-15. In the second case, two methods of impregnation were tested: incipient wetness and excess solvent impregnation. We have seen that the method of impregnation of Al-SBA-15 support by silver nitrate has an influence on the size and location of particles. This difference was observed by various techniques of characterization (XRD, MET, TPR/H_2) and leads to different oxidation properties in the course of $DeNO_x$ process. Ag-SBA-15 support synthesized by one-step hydrothermal synthesis method has well ordered hexagonal mesopores. We showed that it is very difficult to introduce the metal ions into SBA-15 directly due to the difficulties in the formation of metal–O–Si bonds under the strong acidic conditions for the synthesis of SBA-15 materials. A big amount of silver was introduced to obtain 2.5 wt% of metal.

The Ag-SBA-15 materials demonstrate the better oxidation of ethanol into CO and CO_2. The addition of aluminium to Ag-SBA-15 decreases the oxidation of ethanol at high temperatures and simultaneously enhances the reduction of NO_x to N_2.

For the same theoretical molar ratio Si/Al = 10, optimum NO_x reduction activity was observed with Ag/Al-SBA-15 (10) ESI. The low activity of Al/Ag(0.3)-SBA-15 (ESI) and their support is linked

to the low percentage of silver due to the difficulties of the insertion of the metal in the gel of synthesis of SBA-15. The sample Al/Ag(2.5) has higher activity at low temperature but its activity is almost similar to the sample obtained by impregnation. However, to keep a higher $DeNO_x$ activity at low temperatures, the presence of hydrogen in the feed could be the alternative solution.

Acknowledgments

The authors thank Sandra Casale for MET images and Christophe Méthivier for XPS spectroscopy.

Appendix A. Supplementary data

Supplementary data associated with this article can be found, in the online version, at doi:10.1016/j.apcatb.2009.07.004.

References

[1] J.S. Beck, J.C. Vartuli, W.J. Roth, M.E. Leonowicz, C.T. Kresge, K.D. Schmitt, C.T-W. Chu, D.H. Olson, E.W. Sheppard, S.B. McCullen, J.B. Higgins, J.L. Schlenker, J. Am. Chem. Soc. 114 (1992) 10834.
[2] D. Zhao, J. Feng, Q. Huo, N. Melosh, G.H. Fredrickson, B.F. Chmelka, G.D. Stucky, Science 279 (1998) 548.
[3] A. Wingen, F. Kleitz, F. Schüth, Springer Ser. Chem. Phys. 75 (2004) 283.
[4] D.E. De Vos, M. Dams, B.F. Sels, P.A. Jacobs, Chem. Rev. 102 (2002) 3615.
[5] A. Sayari, Chem. Mater. 8 (1996) 1840.
[6] A. Corma, Chem. Rev. 97 (1997) 2373.
[7] J. Perez-Ramirez, F. Kapteijn, K. Schoffel, J.A. Moulijn, Appl. Catal. B 44 (2003) 117.
[8] X. Linag, J. Li, Q. Lin, K. Sun, Catal. Commun. 8 (2007) 1901.
[9] M. Brandhorst, J. Zajac, D.J. Jones, J. Rosière, M. Womes, A. Jimenez-López, E. Rodríguez-Castellón, Appl. Catal. B: Environ. 55 (2005) 267.
[10] J. Huang, Z. Tong, Y. Huang, J. Zhang, Appl. Catal. B: Environ. 78 (2008) 309.
[11] L. Chmielarz, P. Kustrowski, R. Dziembaj, P. Cool, E.F. Vansant, Appl. Catal. B: Environ. 62 (2006) 369.
[12] Y. Segura, L. Chmielarz, P. Kustrowski, P. Cool, R. Dziembaj, E.F. Vansant, Appl. Catal. B: Environ. 61 (2005) 69.
[13] Y. Segura, L. Chmielarz, P. Kustrowski, P. Cool, R. Dziembaj, E.F. Vansant, J. Phys. Chem. B 110 (2006) 948.
[14] M. Iwamato, H. Hamada, Catal. Today 10 (1991) 57.
[15] J.N. Armor, Catal. Today 26 (1995) 99.
[16] M. Iwamato, Catal. Today 29 (1996) 29.
[17] M. Iwamato, H. Frukawa, Y. Mine, F. Uemura, S. Mikuriya, S. Kagawa, J. Chem. Soc. Chem. Commun. (1986) 1272.
[18] R. Brosius, J.A. Martens, Top. Catal. 28 (2004) 119.
[19] D.J. Kim, J.W. Kim, S.-J. Choung, M. Kang, J. Ind. Eng. Chem. 14 (2008) 308.
[20] W. Schieβer, H. Vinek, A. Jentys, Catal. Lett. 56 (1998) 189.
[21] T. Komatsu, K. Tomokuni, I. Yamada, Catal. Today 116 (2006) 244.
[22] S. Kameoka, Y. Ukisu, T. Miyadera, Phys. Chem. Chem. Phys. 2 (2000) 367.
[23] T. Miyadera, K. Yoshida, Chem. Lett. (2000) 294.
[24] S. Sumiya, M. Saito, H. He, Q.C. Feng, N. Takezawa, K. Yoshida, Catal. Lett. 50 (1998) 87.
[25] T. Miyadera, Appl. Catal. B: Environ. 16 (1998) 155.
[26] A. Musi, P. Massiani, D. Brouri, J.M. Trichard, P. Da Costa, Catal. Lett. 128 (2009) 25.
[27] K.T. Campos Roseno, M.A.S. Baldanza, M. Schmal, Catal. Lett. 124 (2008) 59.
[28] M. De Boer, H.M. Huisman, R.J.M. Mos, R.G. Leliveled, A.J. van Dillen, J.W. Geus, Catal. Today 17 (1993) 189.
[29] W.B. Williamson, D.R. Flenige, J.H. Lunsford, J. Catal. 37 (1975) 258.
[30] Y. Li, W. Zhang, Q. Yang, Z. Wie, J. Phys. Chem. B 108 (2004) 9739.
[31] W. Zhu, Y. Han, L. An, Micropor. Mesopor. Mater. 80 (2005) 221.
[32] S. Wu, Y. Han, Y.C. Zou, J.W. Song, L. Zhao, Y. Di, S.Z. Liu, F.S. Xiao, Chem. Mater. 16 (2004) 486.
[33] Maya Boutros, Thesis, University of Pierre et Marie Curie, Paris 6, 2007.
[34] V. Hulea, D. Brunel, A. Galarneau, K. Philippot, B. Chaudret, P.J. Kooyman, F. Fajula, Micropor. Mesopor. Mater. 79 (2005) 185.
[35] M. Boutros, F. Launay, A. Nowicki, T. Onfroy, V. Herledan-Semmer, A. Roucoux, A. Gedeon, J. Mol. Catal. A: Chem. 259 (2006) 91.
[36] M. Richter, M. Langpape, S. Kolf, G. Grubert, R. Eckelt, J. Radnik, M. Schneider, M.-M. Pohl, R. Fricke, Appl. Catal. B: Environ. 36 (2002) 261.
[37] T.-S. Kim, H.S. Kim, T.-G. Kim, H.G. Jeaong, S.-J. Hong, J. Alloys Compd. (2008), doi:10.1016/j.jallcom.2008.07.172.
[38] M. Boutros, J.M. Trichard, P. Da Costa, Top. Catal., 2009, doi:10.1007/s11244-009-9336-8.
[39] R. Burch, J.P. Breen, F.C. Meunier, Appl. Catal. B 39 (2002) 283.
[40] B. Dragoi, E. Dumitriu, C. Guimon, A. Auroux, Micropor. Mesopor. Mater. 121 (2009) 7.
[41] N. Bogdanchikova, F.C. Meunier, M. Avaloj-Borja, J.P. Breen, A. Pestrykov, Appl. Catal. B 36 (2002) 287.
[42] Andrea Musi, Thesis, University of Pierre et Marie Curie, Paris 6, 2008.
[43] F.C. Meunier, J.P. Breen, V. Zuzaniuk, M. Olsson, J.R.H. Ross, J. Catal. 187 (1999) 493.